SPATIAL DISTRIBUTION FEATURES OF PSEUDO VELOCITY RESPONSE FROM THE 2011 OFF THE PACIFIC COAST OF TOHOKU EARTHQUAKE (Mw9.1) AND ITS INTRASLAB AFTERSHOCK (Mw7.1)

Nobuo TAKAI
Hokkaido University , Faculty of Engineering
N13W8 Kita-ku, Sapporo, Hokkaido
JAPAN

Tsutomu SASATANI
Hokkaido University, Faculty of Engineering
N13W8 Kita-ku, Sapporo, Hokkaido
JAPAN

ABSTRACT

A huge interplate earthquake, the 2011 off the Pacific coast of Tohoku Earthquake (Mw9.1) occurred on March 11, 2011. After this earthquake, a large number of aftershocks of diverse earthquake types occurred. One of these aftershocks (Mw7.1) occurring on April 7 was estimated to be an intraslab earthquake. In this study, we calculate pseudo velocity response spectra (damping factor h=0.05) for the two earthquakes and formulate the spatial distribution maps and attenuation relationships. Furthermore, we compare the attenuation relationships with our prediction formula. The spatial distribution maps show different features depending on the natural period. The 0.1sec map shows strong attenuation of the response at the back-arc side of the volcanic front; this can be explained by the heterogeneous S-wave attenuation structure beneath northern Japan. This feature is clearly recognized in the intraslab aftershock and well explained by our prediction formula. The response values for the main shock are larger than for the intraslab aftershock. However, the 0.1sec response values for the aftershock are approximately equivalent to the main shock. This feature indicates different seismic wave radiation depending on the category of earthquake.

INTRODUCTION

The attenuation relation of strong earthquake ground motion, which is predictable in wide areas, is important in earthquake engineering. Many experimental attenuation formulas for estimation of ground motion severity have been developed using regression analysis (e.g., Boore and Joyner, 1982). These formulas are useful in easily predicting strong ground motion and in evaluating newly observed data. However, these are based on a homogenous subsurface structure, therefore the predicted values are distributed on a concentric circle. It is now known that a heterogeneous upper mantle structure exists beneath subduction zones such as those in Japan. This structure causes a region of anomalous seismic intensity in northern Japan. For this region, we have to consider the effects of a heterogeneous structure on the attenuation relation. Recently Kanno et al. (2006) proposed correction terms in the prediction equations of PGA, PGV and acceleration response spectra to take account of a heterogeneous structure. However, their prediction equations still assume a single term of inelastic attenuation.

We proposed new attenuation formulas of pseudo velocity response and PGA taking a heterogeneous structure for interplate and intraslab events [Yadab et al. (2010)]. These formulas consisted of two terms of inelastic attenuation in consideration of a heterogeneous attenuation structure. In these equations, we divided a source-to-site distance into two distances at the attenuation boundary beneath the volcanic front assuming the high Q and low Q zones in the FAMW and BAMW, correspondingly (Figure 1).

The 2011 off the Pacific coast of Tohoku Earthquake (Mw9.1) occurred on March 11, 2011. After this earthquake, a large number of aftershocks of diverse earthquake types occurred. One of these aftershocks (Mw7.1) occurring on April 7 was estimated to be an intraslab earthquake.

The objective of this study is to examine the spatial distribution features of velocity response for the 2011 off the Pacific coast of Tohoku Earthquake and its intraslab aftershock. We formulate the spatial distribution maps and attenuation relations of velocity responses for various natural periods, in order to clarify their period dependence.

DATA AND METHOD

We used strong motion data obtained from the K-NET and KiK-net of National Research Institute for Earth Science and Disaster Prevention (NIED) to examine the spatial distribution of velocity responses in north Japan. The total number of stations used is 1186 for main shock and 813 for intraslab aftershock.

We used pseudo-velocity response spectra to compare with our formulas. First, we calculated 5% damped acceleration response time histories with natural periods of T=0.1, 0.3, 1.0, 3.0, of two horizontal components and took the maximum value from their vector sum history. Second, we divide the maximum value by the angular frequency corresponding to the natural period to obtain the pseudo-velocity response.

Our attenuation formulas are taking a complex Q structure beneath the Japan arc into account. We divided the hypocentral distance (R) at the volcanic front (V.F.) into the high Q fore-arc side mantle wedge (FAMW) side distance (R_1) and the low Q back-arc side mantle wedge (BAMW) side distance (R_2) in order to consider a heterogeneous Q structure (Fig. 1). The V.F. location in northern Japan is shown in Figure 2, 3. We use the ratio of the fore-arc side distance to the hypocentral distance, $R_1/(R_1+R_2=R)$, to simply consider the heterogeneous structure.
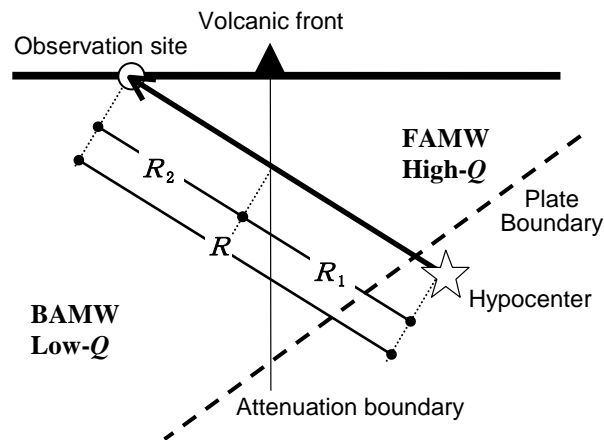

Figure 1. Schematic vertical section of the Japan subduction zone. Definition of distances of R, R_1 and R_2: R is the distance from the hypocenter to the observation site, R_1 is the distance from the hypocenter to the attenuation boundary, and R_2 is the distance from the attenuation boundary to the observation site. FAMW and BAMW denote the fore-arc side and back-arc side mantle wedges, respectively. Q denotes the quality factor.

SPATIAL DISTRIBUTION FEATURES OF VELOCITY RESPONSES

We shows the spatial distribution maps for T=0.1, 0.3, 1.0, and 3sec pseudo-velocity responses. Figure 2 shows the distribution maps of the main shock and Figure 3 shows the maps of the intraslab aftershock. These maps are plotted with focal mechanism distributed by the global CMT project. Concentric circles are epicentral distances at intervals of 100km. These maps show different features depending on the period. In Figures 2 and 3, the response values increase with period all over northern Japan. In the T=0.1 and 0.3sec map, the high response values are located along the Pacific Ocean side, that is, along the FAMW. Even though the area on the Pacific Ocean side of Hokkaido Island was far from the epicenter (more than 500km), a large response was observed. On other hand, in these figures the BAMW has nearly the same low response.

However, except for the T=0.1 and 0.3sec map, the V.F. has no effects on the spatial distributions for T=1.0 and 3.0sec. In T=1.0 and 3.0sec maps in Figures 2 and 3, we can understand that the low land areas were shaken strongly.
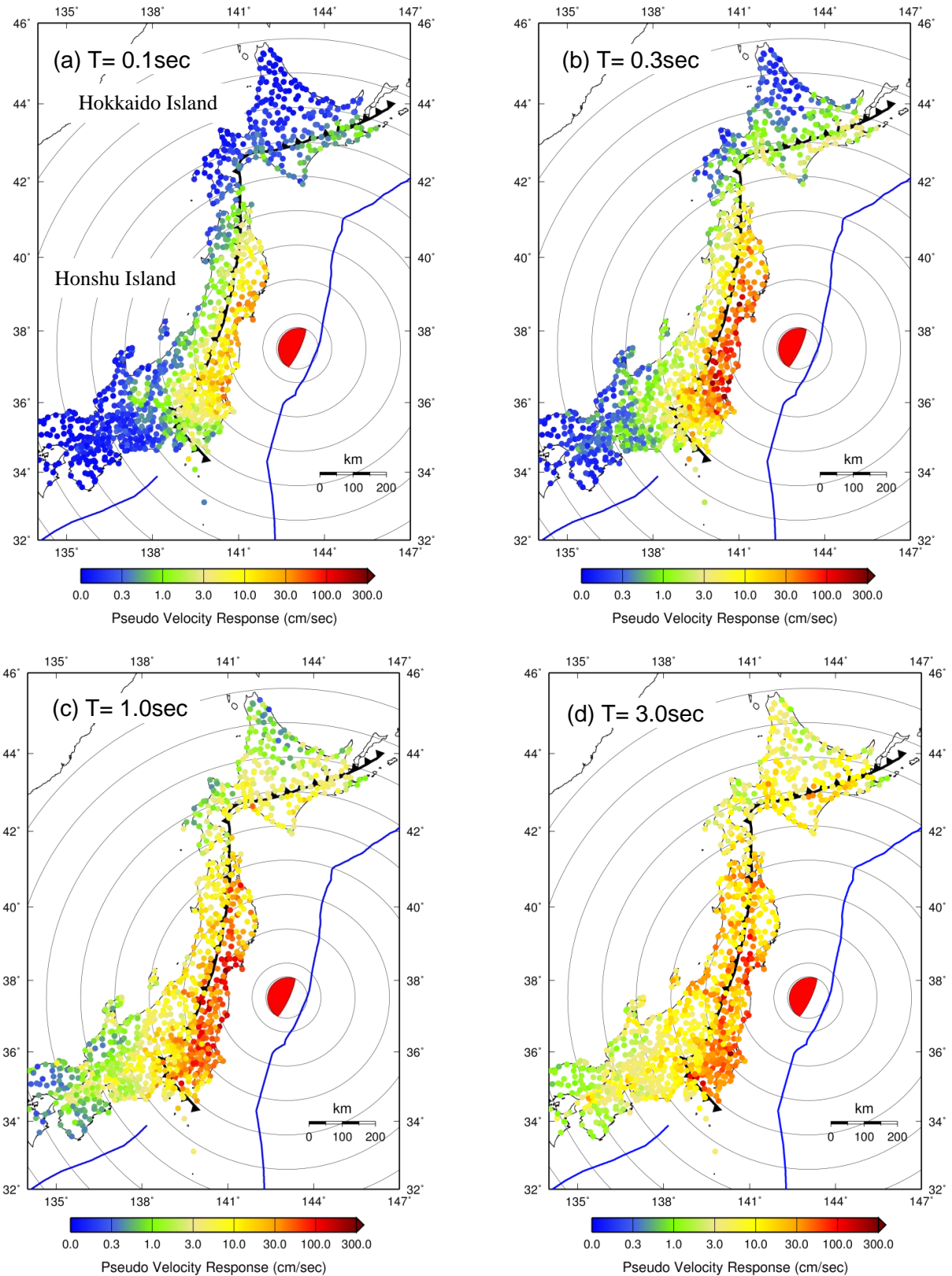
Figure 2. Spatial distribution maps of pseudo-velocity responses during the 2011 off the Pacific coast of Tohoku earthquake (2011 Mar 11 14:46(JST) Mw9.1) for a damping factor of 5% and natural periods of (a) 0.1, (b) 0.3, (c) 1.0 and (d) 3.0sec. Solid blue lines represent the oceanic trench. The black line represents the volcanic front.
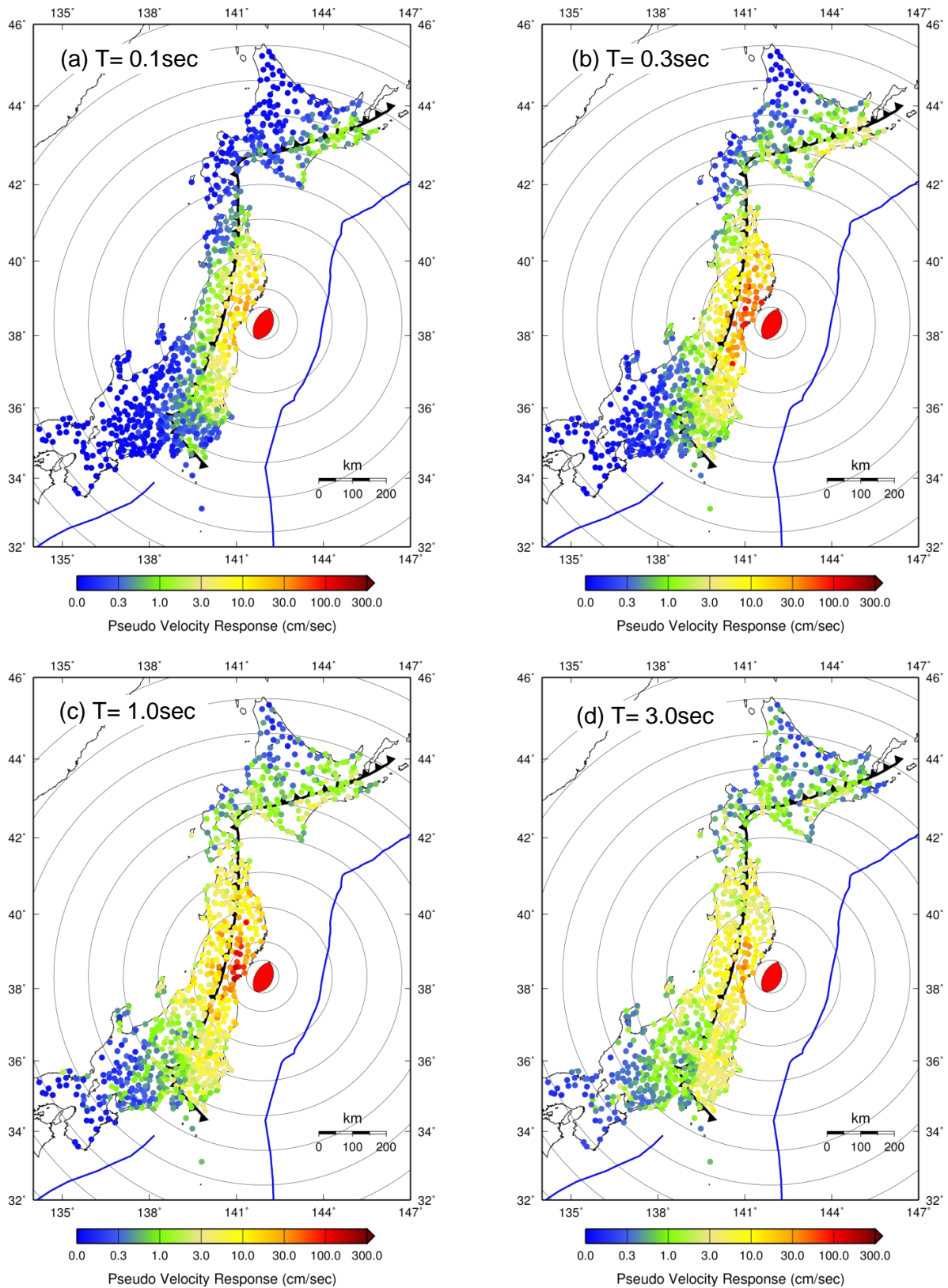
Figure 3. Spatial distribution maps of pseudo-velocity responses during the intraslab aftershock (2011 Apr. 07 23:32(JST) Mw7.1) for a damping factor of 5% and natural periods of (a) 0.1, (b) 0.3, (c) 1.0 and (d) 3.0sec. Solid blue lines represent the oceanic trench. The black line represents the volcanic front.

Figures 4 and 5 show the attenuation relations of the pseudo velocity responses for T=0.1, 0.3, 1.0 and 3.0sec. The data points are classified by a ratio of $R_1/(R_1+R_2)$; the red color means the site was located on the fore-arc side. The scattering of data points decreases with the period. The T=0.1sec relation shows a large scattering over two orders at distances greater than about 300km, while the T=3.0sec relation shows a considerably small scattering. The decay rates also change with the period. We consider that these features result from the seismic source, propagation path and site effects on velocity responses.
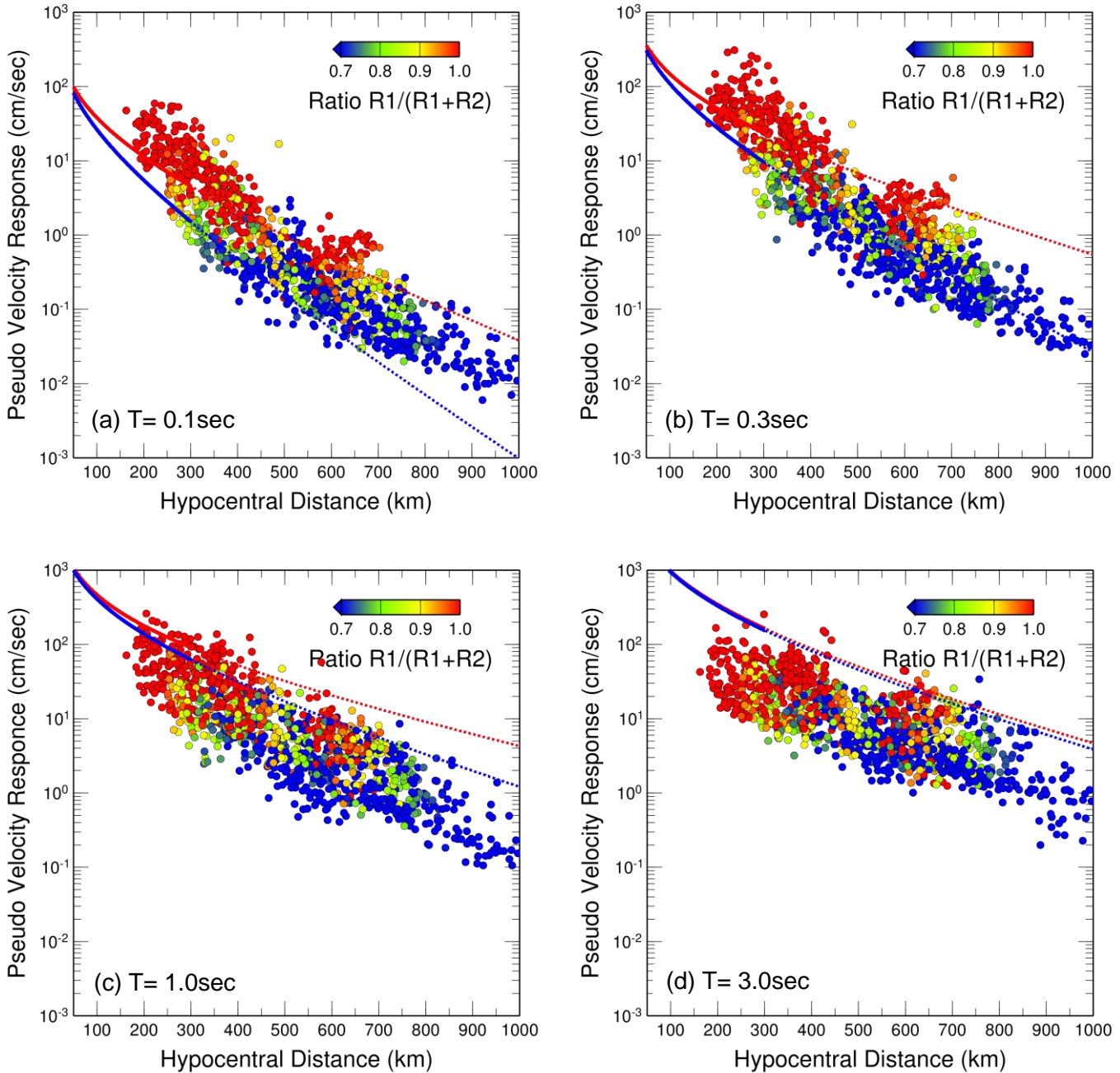

Figure 4. Attenuation relationships of velocity responses during the 2011 off the Pacific coast of Tohoku earthquake (2011 Mar 11 14:46(JST) Mw9.1) for a damping factor of 5% and natural periods of (a) 0.1, (b) 0.3, (c) 1.0 and (d) 3.0sec. The data points are classified by a ratio of $R_1/(R_1+R_2)$. Solid red and blue lines are Yadab et al.'s formulas for ratios 1.0 and 0.7, and the dashed lines are formulas extended by extrapolation.

The variety of the response level at 500-700km is larger in the intraslab aftershock than in the main shock. These observation sites are located on the Pacific Ocean side of Hokkaido. At that distance range, in spite of Mw7.1, the response levels are the same as or higher than the response levels of the Mw9.1 main shock. However, high level responses in this area are hidden over T=1.0sec. It is expected that the intraslab earthquake generated high level short period seismic waves and the Pacific plate guided them.

The response values of the main shock and our formulas are relatively equal at 0.3sec, but not equal in other periods. Therefore, we took the fault distances on the x axis because the Mw9.1 main shock had a very wide fault plane (Figure 6). We use the fault plane predicted by Shao etal (2011). However, the consistency turned out even worse. We think that it is necessary to examine the places that generate strong motion at each frequency in detail. On the other hand, the predicted and the observed values have high consistency in the intraslab aftershock, except at the Pacific Ocean side of Hokkaido located 500-700km from epicenter. For the Pacific Ocean side of Hokkaido, it is necessary to examine the influence of the path effect in more detail.
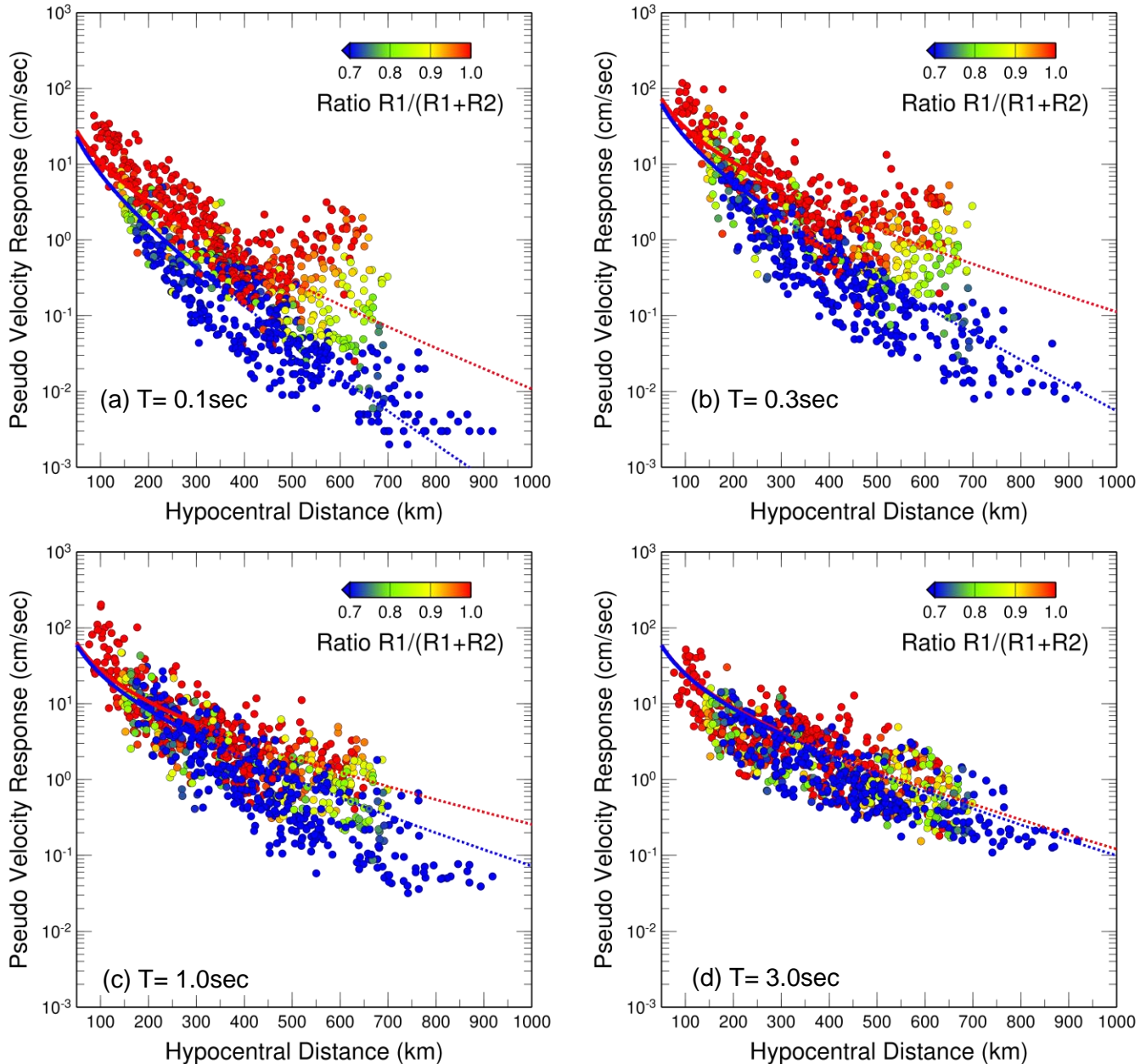

Figure 5. Attenuation relationships of velocity responses during the intraslab aftershock (2011 Apr. 07 23:32(JST) Mw7.1) for a damping factor of 5% and natural periods of (a) 0.1, (b) 0.3, (c) 1.0 and (d) 3.0sec. The data points are classified by a ratio of $R_1/(R_1+R_2)$. Solid red and blue lines are Yadab et al.'s formulas for ratios 1.0 and 0.7, and the dashed lines are formulas extended by extrapolation.
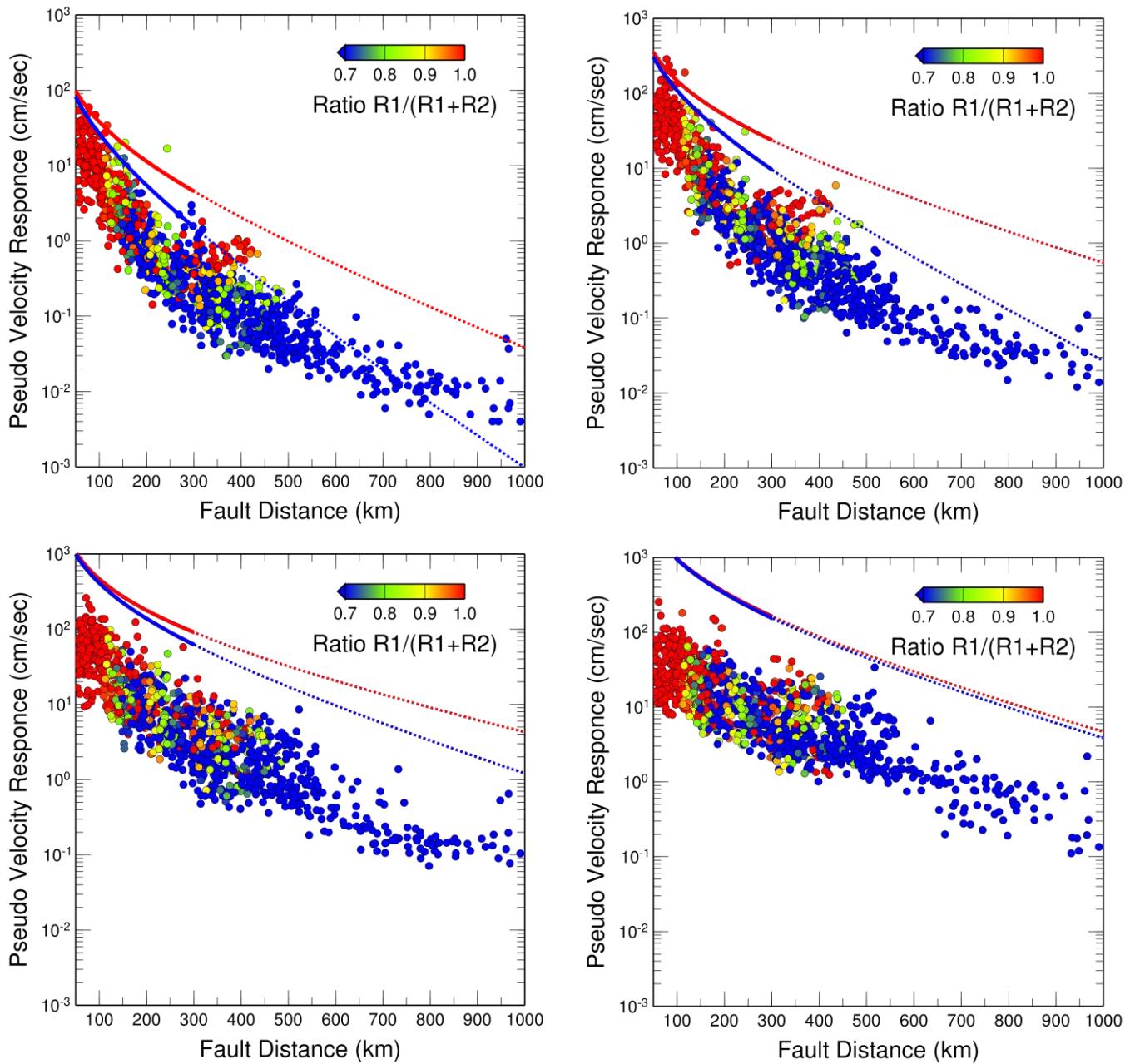
Figure 6. Attenuation relationships of velocity responses versus fault distances during the 2011 off the Pacific coast of Tohoku earthquake (2011 Mar 11 14:46(JST) Mw9.1) for a damping factor of 5% and natural periods of (a) 0.1, (b) 0.3, (c) 1.0 and (d) 3.0sec. The data points are classified by a ratio of $R_1/(R_1+R_2)$. Solid red and blue lines are Yadab et al.'s formulas for ratios 1.0 and 0.7, and the dashed lines are formulas extended by extrapolation.

COMPARING RESIDUALS AND AVS30

Correlation is high in residuals which removed the seismic source and the path effect and the value of AVS30 (the average shear-wave velocity) at site, in over T=0.5sec (Kanno et al., 2006). Therefore, in these two earthquakes, we compared the ratio of our formulas and the observed values with AVS30 for within 300km hypocentral distance data (Figure 7). Low correlation is seen at T=0.1 and 0.3sec in both earthquakes, and it is thought that this is caused by that these short period response values are affected by shallow underground conditions. About over 300km hypocentral distance data, prediction equations being unable to evaluate the pass effects enough. At T=1.0 an 3.0sec, as the values of AVS30 increase residuals are small, therefore it can be understood that the response levels depend on the surface soil conditions.
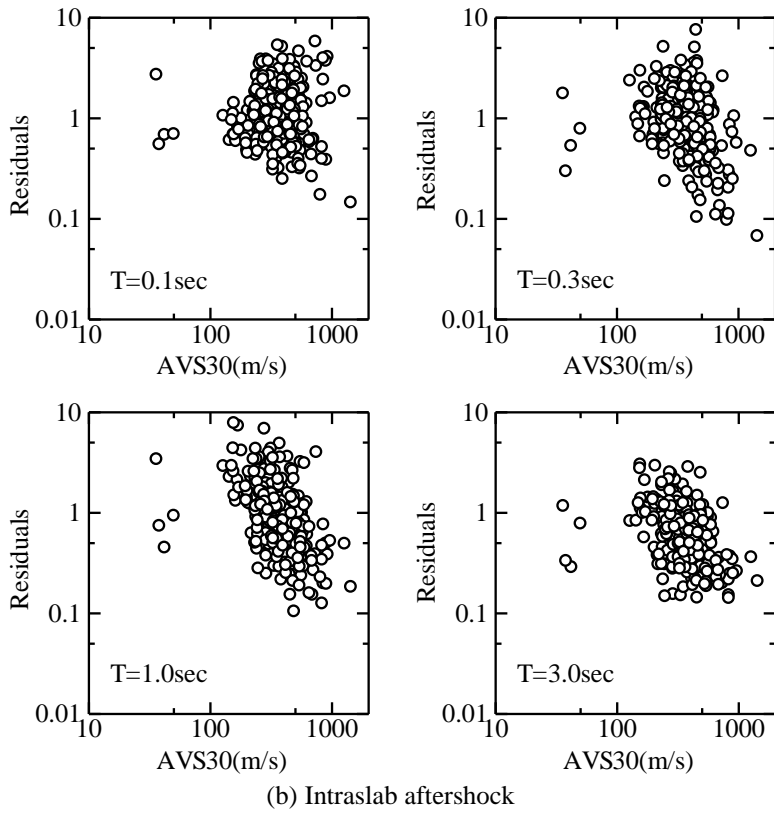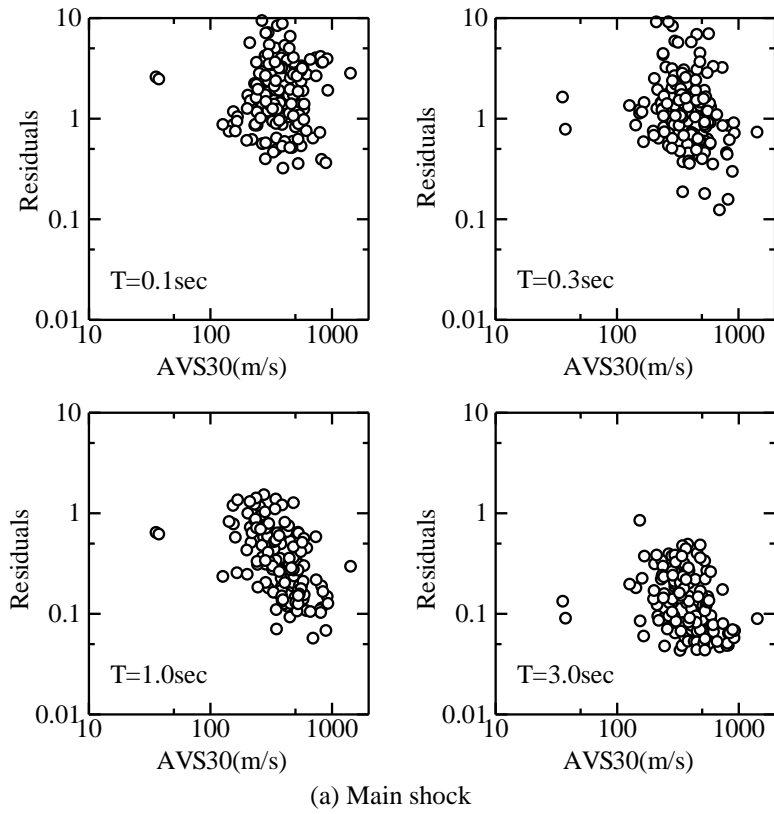
7

(a) Main shock

(b) Intraslab aftershock

Figure 7. Relation between AVS30 and residual of observed responses (observed/predicted) from formulas.
(a) Main shock, (b) Intraslab aftershock for within 300km hypocentral distance data.

CONCLUSION

We have examined pseudo velocity responses based on strong ground motion data from the 2011 off the Pacific coast of Tohoku Earthquake (Mw9.1) and its intraslab aftershock (Mw7.1). We formulated spatial distribution maps and attenuation relations of pseudo velocity responses (damping factor h=0.05) for various natural periods. We found that the short-period (T~0.1sec) distribution maps and attenuation relations are mainly controlled by the path effect due to heterogeneous Q structure beneath the northern Japan arc, and that the long-period (T~3sec) maps and relations are in part controlled by the surface structure.

Our formulas are compared with observed responses. Especially for intraslab aftershock, tendency of observed values are clearly explained by our formulas in short periods range.

By taking these findings into account, we try to upgrade the prediction method of a wide-band and wide distance, high-precision response spectrum for a large earthquake.

ACKNOWLEDGMENTS

REFERENCES

Boore, D.M, and Joyner W.B [1982], "The empirical prediction of ground motion" Bull. Seism. Soc. Am., Vol.72, No. 1, S43-S60.

Kanno et al. [2006], "A New Attenuation Relation for Strong Ground Motion in Japan Based on Recorded Data", Bull. Seism. Soc. Am., Vol. 96, No. 3, pp. 879–897.

Shao Guangfu, Xiangyu Li, Chen Ji and Takahiro Maeda [2011], "Preliminary Result of the Mar 11, 2011 Mw 9.1 Honshu Earthquake", URL: http://www.geol.ucsb.edu/faculty/ji/big_earthquakes/2011/03/0311_v2/Honshu_2.html

Wessel, P. and W. H. F. Smith [1991], Free software helps map and display data, EOS Trans. AGU, 72, 441.

Yadab P. Dhakal, Nobuo Takai and Tsutomu Sasatani. [2010], "Empirical analysis of path effects on prediction equations of pseudo-velocity response spectra in northern Japan", Earthquake Engng Struct. Dyn. 2010; 39:443–461.